

Adsorption Equilibria of Water Vapor on Alumina, Zeolite 13X, and a Zeolite X/Activated Carbon Composite

Jong-Hwa Kim,[†] Chang-Ha Lee,^{*,†} Woo-Sik Kim,[†] Jong-Seok Lee,[‡] Jin-Tae Kim,[‡]
Jeong-Kwon Suh,[‡] and Jung-Min Lee[‡]

Department of Chemical Engineering, Yonsei University, Seoul 120-749, Korea, and Applied Chemistry & Engineering Division, Korea Research Institute of Chemical Technology, Taejeon 305-600, Korea

The adsorption equilibria of water vapor on Al₂O₃, zeolite 13X, and a zeolite X/activated carbon composite (Zeocarbon) were measured by a static volumetric method. The equilibrium experiments were conducted at (293.2, 313.2, 333.1, and 353.1) K and pressures up to 2.1 kPa for Al₂O₃ and 2.3 kPa for zeolite 13X and Zeocarbon, respectively. The experimental data obtained were correlated by the Aranovich and Donohue (A–D) and *n*-layer BET models.

Introduction

Adsorption of gases and vapors by microporous solids has attracted much attention because of its great practical importance in the fields of gas separation, gas purification, and environmental problems. Information concerning adsorption equilibria is used to calculate the operation time of a specific bulk concentration level and to derive the optimum size of adsorbents and operating conditions.⁴

An issue that has come under increasing scrutiny in recent years is the interaction between water vapor and adsorbents.¹ Also, the need for moisture removal technology is becoming greater, as product quality issues caused by moisture occur frequently.² Adsorption of water vapor has been encountered in applications such as VOC removal from humid air streams, the steam regeneration process, and the adsorption drying process.

To estimate practical or dynamic adsorption capacity, however, it is essential to have information on the adsorption equilibrium.³ Furthermore, it is important to select the proper adsorbent for the design of an efficient adsorption process. The selection of a proper adsorbent for a given separation is a complex problem. The predominant scientific basis for adsorbents is the equilibrium isotherm,⁴ and thermodynamic data on adsorption equilibria must be known over a wide range of temperatures.

In this study, the commercial adsorbents for Al₂O₃, zeolite 13X, and Zeocarbon were used in the experiments for the adsorption equilibrium of water vapor. Alumina and zeolite 13X, chosen as adsorbents, are the most common adsorbents today, exhibiting large adsorption capacities of water vapor because of their hydrophilic property, large surface area, and the greatest affinity for water.⁴ Also, a zeolite X/activated carbon composite (Zeocarbon) synthesized from rice hulls and in pelletized form was selected as an adsorbent because Zeocarbon is a new adsorbent, having characteristics of both zeolite and activated carbon such as high hydrophilic property, high adsorption of polar molecules, and hydrophobic efficiency for adsorption of nonpolar molecules, respectively.⁵ Until quite recently,

Table 1. Physical Properties of Al₂O₃ (1) + Zeolite 13X (2) + Zeocarbon (3)

property	Al ₂ O ₃	zeolite 13X	Zeocarbon
bulk density/kg·m ⁻³	810	689	500
BET surface area/m ² ·g ⁻¹	340	726	620
micropore area/m ² ·g ⁻¹	137	678	467
micropore vol/cm ³ ·g ⁻¹	0.14	0.25	0.19
BJH desorption avg pore diam/nm	34	28	27
avg pore diam by BET/nm	51	23	28

there was not a great deal of reliable information concerning the adsorption of water vapor on Zeocarbon. Given this situation, the adsorption isotherms for water vapor on Zeocarbon were compared with those for water vapor on Al₂O₃ and zeolite 13X. The experimental data obtained at various temperatures were correlated with existing adsorption isotherm models such as the Aranovich–Donohue (A–D) and *n*-layer BET models.

Experimental Section

Materials. Spherical Al₂O₃, zeolite 13X, and Zeocarbon were supplied by Procatalyze Co., Aldrich Co., and Zeobuilder Co., respectively. Zeocarbon synthesized from rice hulls consists of the following components: 38.5 mass % zeolite X, 35 mass % activated carbon, 10 mass % inert silica, and 16.5 mass % zeolites A and P. The zeolite in Zeocarbon was exchanged with Ca ion by the supplier.⁵ Both adsorbent samples were crushed to 20–30 mesh. Prior to measurement, all the adsorbents were kept in a drying vacuum oven at 423.0 K for more than 24 h to remove impurities. The BET surface area, micropore volume, and pore diameter of the adsorbents were measured with an automatic volumetric sorption analyzer (Micromeritics, ASAP-2010) using nitrogen adsorption at 77.0 K. The measured and supplied physical properties of the Al₂O₃, zeolite 13X, and Zeocarbon are listed in Table 1.

Apparatus and Procedure. The adsorption experimental apparatus used was a static volumetric system, and a schematic diagram of the apparatus is shown in Figure 1. The total quantity of gas admitted into the system and the amount of gas in the vapor phase remaining after adsorption equilibrium were determined by appropriate *P–V–T* measurements.

* To whom correspondence should be addressed. Telephone: +82-2-2123-2762. Fax: +82-2-2123-6401. E-mail: leech@yonsei.ac.kr.

[†] Yonsei University.

[‡] Korea Research Institute of Chemical Technology.

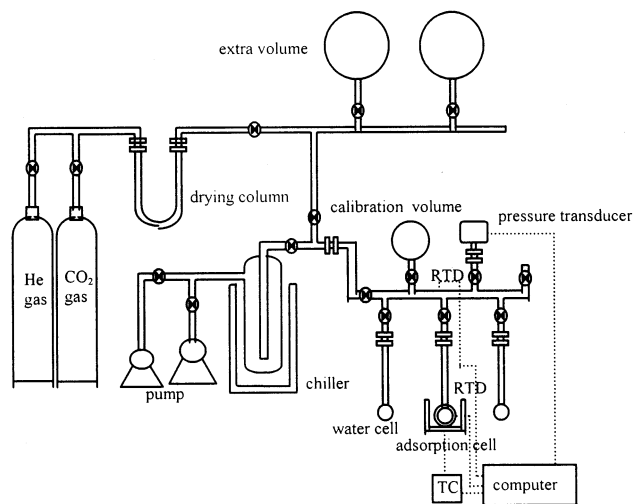


Figure 1. Adsorption equilibrium apparatus.

The system pressure was measured by an absolute pressure transducer (MKS, type 690A13TRA) with a high-accuracy signal conditioner (MKS, type 270D). Its pressure range is from 0 to 133.33 kPa, and its reading uncertainty is $\pm 0.05\%$ within the usable measurement range. A RTD (Pt 100 Ω) was installed inside the adsorption cell. During experiments, the adsorption cell was placed in a water bath and the temperature was maintained constant to within ± 0.02 K with a refrigerating circulator (Haake type F3). To prevent the water vapor from turning into condensation, the temperature of the manifold in the system was kept constant at 303.1 K with a heating tape. Also, the maximum limit of the experimental pressure was determined by the lower than saturated pressure of water vapor at this temperature.

The mass of all samples was determined with a microbalance with an accuracy of ± 10 μg , and the samples were put into the adsorption cell. Prior to each isotherm measurement, the charged adsorbents were regenerated at 593.1 K under a high vacuum for more than 12 h. An oil diffusion pump and a mechanical vacuum pump in combination (Edwards type Diffstak 63/150M) provided a vacuum down to 10^{-3} Pa, and the evacuation was monitored with a pressure indicator. The volumes of the manifold and adsorption cell in the adsorption system were determined by the expansion of helium gas at the experimental temperature.

Details of the equipment and the operating procedures used are described in a previous work.⁶

Results and Discussion

In this study, the adsorption isotherm data for water vapor on Al_2O_3 , zeolite 13X, and Zeocarbon were obtained at (293.2, 313.2, 333.1, and 353.1) K and pressures up to 2.1 kPa for Al_2O_3 and 2.3 kPa for zeolite 13X and Zeocarbon, respectively.

The adsorption isotherms for water vapor on Al_2O_3 , zeolite 13X, and Zeocarbon at the various temperatures are shown in Figures 2–4, and the data are presented in Tables 2–4. At 293.2 K, the adsorption isotherms of water vapor for all adsorbents used are type II isotherms of the Brunauers classification, having a noticeable uptake (or showing multilayer adsorption) near the relative pressure $P/P_s = 0.36, 0.86,$ and 0.74 on Al_2O_3 , zeolite 13X, and Zeocarbon, respectively. However, the others at the other

Table 2. Adsorption Isotherm Data for Water Vapor on Al_2O_3

P	q	P	q	P	q	P	q
kPa	$\text{mol}\cdot\text{kg}^{-1}$	kPa	$\text{mol}\cdot\text{kg}^{-1}$	kPa	$\text{mol}\cdot\text{kg}^{-1}$	kPa	$\text{mol}\cdot\text{kg}^{-1}$
293.2 K				313.2 K			
0.023	1.054	1.139	6.710	0.012	1.029	1.317	4.240
0.065	2.156	1.352	7.601	0.132	2.189	1.725	4.787
0.267	3.189	1.560	8.655	0.416	2.892	2.177	5.341
0.499	3.991	1.780	9.853	0.597	3.224	2.373	5.617
0.689	4.646	1.869	10.83	0.855	3.641		
0.833	5.241	2.021	12.02				
0.988	5.928	2.096	13.14				
333.1 K				353.1 K			
0.012	0.861	1.459	3.029	0.036	1.018	1.233	2.151
0.264	1.886	1.647	3.143	0.368	1.602	1.508	2.271
0.603	2.272	1.763	3.216	0.633	1.824	1.791	2.381
0.793	2.447	1.915	3.278	0.864	1.954	2.096	2.495
0.961	2.594	2.035	3.334	1.012	2.039	2.304	2.599
1.099	2.728	2.149	3.394				
1.296	2.860	2.293	3.488				

Table 3. Adsorption Isotherm Data for Water Vapor on Zeolite 13X

P	q	P	q	P	q	P	q
kPa	$\text{mol}\cdot\text{kg}^{-1}$	kPa	$\text{mol}\cdot\text{kg}^{-1}$	kPa	$\text{mol}\cdot\text{kg}^{-1}$	kPa	$\text{mol}\cdot\text{kg}^{-1}$
293.2 K				313.2 K			
0.004	3.158	1.265	1.565	0.009	4.599	1.639	11.04
0.007	5.140	1.731	12.56	0.039	7.452	1.887	11.20
0.020	7.442	1.855	12.78	0.481	9.676	2.131	11.35
0.188	9.728	2.013	13.08	1.167	10.70		
0.603	0.736	2.156	13.53				
0.851	1.101	2.220	13.97				
1.060	1.361	2.276	14.29				
333.1 K				353.1 K			
0.035	4.078	1.663	9.608	0.092	3.925	1.505	8.246
0.165	6.925	1.777	9.702	0.395	6.257	1.747	8.424
0.660	8.649	2.031	9.854	0.872	7.511	1.992	8.585
1.162	9.233	2.289	9.995	1.232	8.001	2.231	8.717
1.459	9.470						

Table 4. Adsorption Isotherm Data for Water Vapor on Zeocarbon

P	q	P	q	P	q	P	q
kPa	$\text{mol}\cdot\text{kg}^{-1}$	kPa	$\text{mol}\cdot\text{kg}^{-1}$	kPa	$\text{mol}\cdot\text{kg}^{-1}$	kPa	$\text{mol}\cdot\text{kg}^{-1}$
293.2 K				313.2 K			
0.001	3.015	1.491	8.613	0.008	3.225	1.277	6.781
0.004	3.892	1.717	9.197	0.040	4.501	1.464	6.928
0.053	5.101	1.949	9.863	0.240	5.545	1.677	7.063
0.279	6.174	2.111	10.46	0.588	6.154	2.016	7.228
0.603	6.842	2.189	10.89	0.859	6.459	2.204	7.378
0.851	7.287	2.240	11.25	1.053	6.646	2.317	7.444
1.060	7.699	2.267	11.53				
1.265	8.106						
333.1 K				353.1 K			
0.008	1.329	1.621	5.342	0.047	1.653	1.631	4.490
0.057	2.836	1.756	5.432	0.265	2.990	1.804	4.573
0.329	4.167	1.897	5.509	0.656	3.718	1.911	4.649
0.829	4.765	2.029	5.586	0.979	4.009	2.055	4.693
1.144	5.009	2.157	5.671	1.193	4.191	2.168	4.762
1.335	5.150	2.313	5.729	1.371	4.306	2.301	4.828
1.489	5.244			1.524	4.414		

experimental temperatures were type I due to low relative pressure. Also, as shown in Figures 2–4 the order of the adsorption capacity of water vapor on Al_2O_3 , zeolite 13X, and Zeocarbon was on zeolite 13X, Zeocarbon, and Al_2O_3 within the experimental range. However, the adsorption capacity of Al_2O_3 was larger than that of Zeocarbon at 293.2 K and in the high-pressure range. Zeolite 13X in Figure 3 showed the most favorable isotherm in the low-pressure range because the affinity of water-vapor adsorption in zeolite 13X is higher than that in Zeocarbon and Al_2O_3 .

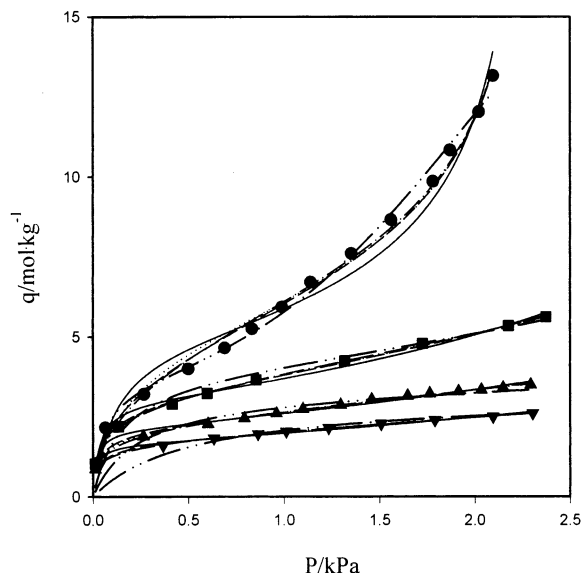


Figure 2. Experimental and correlated isotherms for water vapor adsorption onto Al_2O_3 at various temperatures: ●, 293.2 K; ■, 313.2 K; ▲, 333.1 K; ▼, 353.1 K; —, A–D equation for $f(P)$ = Langmuir equation; - - -, A–D equation for $f(P)$ = Toth equation; ⋯, A–D equation for $f(P)$ = UNILAN equation; ···, A–D equation for $f(P)$ = Sips equation; ····, n -layer BET equation.

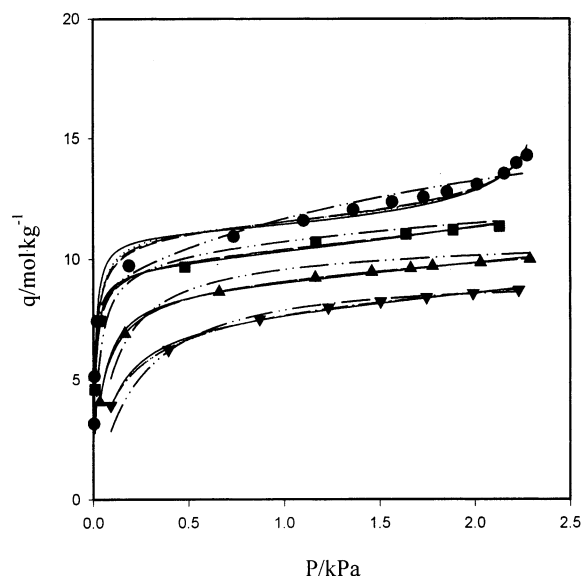


Figure 3. Experimental and correlated isotherms for water vapor adsorption onto zeolite 13X at various temperatures: ●, 293.2 K; ■, 313.2 K; ▲, 333.1 K; ▼, 353.1 K; —, A–D equation for $f(P)$ = Langmuir equation; - - -, A–D equation for $f(P)$ = Toth equation; ⋯, A–D equation for $f(P)$ = UNILAN equation; ···, A–D equation for $f(P)$ = Sips equation; ····, n -layer BET equation.

The adsorption isotherm of Zeocarbon in Figure 4 also was more favorable than that of Al_2O_3 in Figure 2. Moreover, the isotherm shape of Zeocarbon was similar to that of zeolite 13X while the adsorption capacity was smaller than that of zeolite 13X, owing to the content of the activated carbon in Zeocarbon.

Aranovich–Donohue (A–D) Equation. The characteristic feature of multilayer adsorption isotherm type II in the international classification scheme is a sigmoidal shape with an apparent divergence of q to infinity as P approaches P_s . Hence, the mathematical function used to describe the isotherm curve must have a singularity at P equal to the saturation pressure, P_s . Aranovich and Dono-

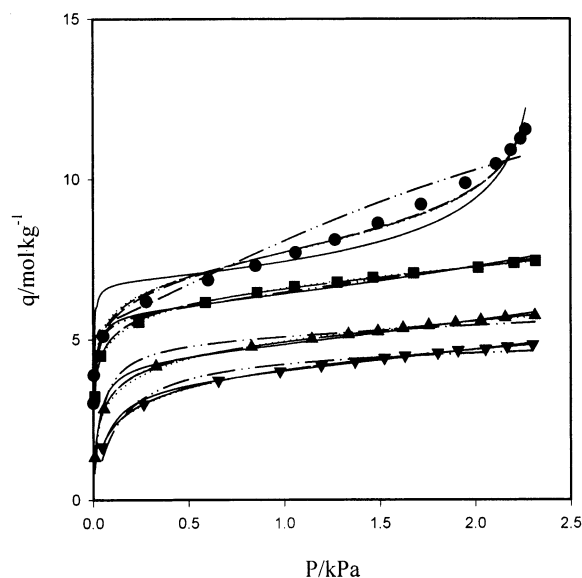


Figure 4. Experimental and correlated isotherms for water vapor adsorption onto Zeocarbon at various temperatures: ●, 293.2 K; ■, 313.2 K; ▲, 333.1 K; ▼, 353.1 K; —, A–D equation for $f(P)$ = Langmuir equation; - - -, A–D equation for $f(P)$ = Toth equation; ⋯, A–D equation for $f(P)$ = UNILAN equation; ···, A–D equation for $f(P)$ = Sips equation; ····, n -layer BET equation.

hue⁷ proposed an isotherm model of the following form:

$$q = f(P)/(1 - P/P_s)^d \quad (1)$$

Here, q is adsorbed moles and the term $1/(1 - P/P_s)^d$ describes the singularity. Given the definition of $f(P)$, the monolayer capacity q_m can be determined as $f(P_s)$ because $f(P_s)$ corresponds to the maximum monolayer adsorption. By substituting $f(P)$ with the Langmuir, Toth, UNILAN, or Sips equation,⁸ eq 1 can be expressed as

for $f(P)$ = Langmuir equation

$$q = \frac{q_m b P}{(1 + bP)(1 - P/P_s)^d} \quad (2)$$

for $f(P)$ = Toth equation

$$q = \frac{q_m P}{(b + P)^{1/t}(1 - P/P_s)^d} \quad (3)$$

for $f(P)$ = UNILAN equation

$$q = \frac{q_m \ln \left[\frac{c + P e^{+s}}{c + P e^{-s}} \right]}{2s(1 - P/P_s)^d} \quad (4)$$

for $f(P)$ = Sips equation

$$q = \frac{q_m (bP)^{1/n}}{(1 + (bP)^{1/n})(1 - P/P_s)^d} \quad (5)$$

where q_m , b , t , c , s , n , and d are isotherm parameters which are numerically determined. In this study, a nonlinear curve-fitting procedure was used to determine parameters. The parameters obtained from the best fit to experimental data are summarized in Tables 5–8 with the average percent deviations, Δq_1 , and the degree of dispersion, Δq_2 ,

Table 5. A–D Equation Parameters for Water on Al₂O₃ (1) + Zeolite 13X (2) + Zeocarbon (3) for $f(P)$ = Langmuir Equation

adsorbent	T	q_m	b	d	Δq_1	Δq_2
	K	mol·kg ⁻¹	kPa		%	%
Al ₂ O ₃	293.2	5.036	8.780	0.472	8.90	4.25
	313.2	2.944	31.79	1.759	5.78	1.15
	333.1	2.100	52.91	4.466	2.86	0.30
	353.1	1.626	60.32	9.966	2.99	0.22
zeolite 13X	293.2	11.04	110.0	0.081	3.24	1.40
	313.2	9.652	93.72	0.527	1.32	0.18
	333.1	8.802	23.78	1.258	0.87	0.09
	353.1	7.780	10.50	3.428	1.15	0.13
Zeocarbon	293.2	6.776	412.5	0.169	7.75	5.75
	313.2	5.828	131.4	0.712	3.28	0.72
	333.1	4.386	39.66	2.397	3.03	0.62
	353.1	3.791	15.15	5.660	1.37	0.10

Table 6. A–D Equation Parameters for Water on Al₂O₃ (1) + Zeolite 13X (2) + Zeocarbon (3) for $f(P)$ = Toth Equation

adsorbent	T	q_m	b	t	d	Δq_1	Δq_2
	K	mol·kg ⁻¹	kPa			%	%
Al ₂ O ₃	293.2	88.64	144.2	0.1407	0.3250	4.60	1.20
	313.2	4.875	179.5	0.3510	1.214	1.70	0.09
	333.1	2.788	186.9	0.4321	3.311	3.12	0.18
	353.1	2.089	209.5	0.4539	7.070	1.03	0.03
zeolite 13X	293.2	11.66	226.3	0.6386	0.0693	3.53	1.52
	313.2	10.07	141.0	0.7669	0.4231	0.96	0.11
	333.1	9.654	34.68	0.7284	0.7502	0.08	0.00
	353.1	7.775	10.48	1.002	3.437	1.15	0.13
Zeocarbon	293.2	16.46	1.758 × 10 ⁸	0.1195	0.1208	2.77	0.68
	313.2	8.173	1.052 × 10 ⁴	0.2778	0.3143	0.55	0.03
	333.1	5.523	121.2	0.4905	1.332	0.25	0.00
	353.1	5.120	35.01	0.5012	2.746	0.23	0.00

Table 7. A–D Equation Parameters for Water on Al₂O₃ (1) + Zeolite 13X (2) + Zeocarbon (3) for $f(P)$ = UNILAN Equation

adsorbent	T	q_m	c	s	d	Δq_1	Δq_2
	K	mol·kg ⁻¹	kPa			%	%
Al ₂ O ₃	293.2	12.71	2.648	4.472	0.3551	6.78	2.62
	313.2	10.28	37.44	9.763	1.102	1.36	0.06
	333.1	7.228	44.95	10.59	2.515	2.29	0.10
	353.1	5.548	50.00	11.32	5.062	0.55	0.01
zeolite 13X	293.2	11.26	0.0101	1.994	0.0744	3.71	1.64
	313.2	9.813	0.0108	1.370	0.475	0.80	0.78
	333.1	9.272	0.0467	1.683	0.878	0.11	0.10
	353.1	8.954	0.131	2.143	1.562	0.40	0.02
Zeocarbon	293.2	10.80	0.0602	8.462	0.124	2.75	0.69
	313.2	10.38	0.144	7.978	0.157	0.71	0.06
	333.1	9.179	0.681	6.157	0.289	1.20	0.08
	353.1	8.802	1.709	5.589	0.775	0.40	0.01

calculated by the following equations:

$$\Delta q_1/\% = \frac{100}{k} \sum_{j=1}^k \left| \frac{q_j^{\text{exp}} - q_j^{\text{cal}}}{q_j^{\text{exp}}} \right| \quad (6)$$

$$\Delta q_2/\% = \frac{100}{k} \sum_{j=1}^k \frac{[q_j^{\text{exp}} - q_j^{\text{cal}}]^2}{q_j^{\text{exp}}} \quad (7)$$

where k is the number of data points at a given temperature and q^{exp} and q^{cal} are the experimental and calculated adsorbed moles, respectively. The solid, short dash, dotted, and dash-dot lines in Figures 2–4 denote the calculated adsorption isotherms from the A–D equation, substituting $f(P)$ with the Langmuir, Toth, UNILAN, and Sips equations, respectively. As shown in Figures 2–4, the experimental data were well fitted by the calculated isotherms for Al₂O₃, zeolite 13X, and Zeocarbon, especially by using the A–D equation with the Sips equation. The A–D model

Table 8. A–D Equation Parameters for Water on Al₂O₃ (1) + Zeolite 13X (2) + Zeocarbon (3) for $f(P)$ = Sips Equation

adsorbent	T	q_m	b	n	d	Δq_1	Δq_2
	K	mol·kg ⁻¹	kPa			%	%
Al ₂ O ₃	293.2	14.471	0.3207	1.878	0.3198	4.73	1.56
	313.2	6.989	0.7815	2.685	0.9482	0.87	0.03
	333.1	4.912	0.8209	2.942	2.109	1.56	0.05
	353.1	3.689	0.9620	3.433	4.665	0.45	0.01
zeolite 13X	293.2	11.47	94.28	1.349	0.0717	3.31	1.62
	313.2	9.917	90.98	1.168	0.4546	0.81	0.10
	333.1	9.509	20.11	1.253	0.7982	0.09	0.00
	353.1	9.239	7.005	1.379	1.528	0.46	0.02
Zeocarbon	293.2	16.99	0.1943	5.461	0.1168	2.35	0.52
	313.2	7.494	63.31	2.578	0.3449	0.61	0.03
	333.1	5.165	23.48	1.576	1.493	0.16	0.00
	353.1	4.957	6.958	1.615	2.801	0.17	0.00

Table 9. N-layered BET Equation Parameters for Water on Al₂O₃ (1) + Zeolite 13X (3) + Zeocarbon (3)

adsorbent	T	q_m	c	n	Δq_1	Δq_2
	K	mol·kg ⁻¹			%	%
Al ₂ O ₃	293.2	3.424	49.23	7.376	2.99	0.67
	313.2	3.906	51.56	16.00	12.2	6.67
	333.1	3.206	88.10	64.33	18.1	9.28
	353.1	2.953	101.0	84.33	11.6	7.04
zeolite 13X	293.2	10.99	199.6	0.441	4.07	1.79
	313.2	10.21	210.4	1.172	9.75	13.98
	333.1	9.985	302.2	1.685	6.45	4.12
	353.1	8.925	418.5	2.056	4.47	3.83
Zeocarbon	293.2	5.410	1881	3.009	4.83	2.29
	313.2	5.696	1042	2.575	2.46	0.47
	333.1	4.988	502.7	2.495	5.65	1.99
	353.1	4.651	373.4	2.176	4.90	1.22

provided a better isotherm fit at higher temperatures than the n -layer BET model did at 293.2 K for all adsorbents. Also, the deviation of all the isotherm equations was much larger at lower pressures than that at higher pressures.

BET Equation for n -Layers. When the adsorption space is finite in the case of the finite size of pores, that is when the adsorption layer is limited by n -layers, the n -layer BET equation can be described by the following form.⁸

$$\frac{q}{q_m} = \frac{C(P/P_s)}{1 - (P/P_s)} \frac{1 - (n+1)(P/P_s)^n + n(P/P_s)^{n+1}}{1 + (C-1)(P/P_s) - C(P/P_s)^{(n+1)}} \quad (8)$$

where q_m , C , and n are isotherm parameters. When n approaches infinity, this equation reduces to the classical BET equation. The parameter C is normally greater than 1 because the heat of adsorption of the first layer is greater than the heat of liquefaction; that is, the attractive forces between the adsorbed molecule and the adsorbent are greater than the attractive forces between molecules in the liquid state. The parameters, average percent deviations, and the degree of dispersion calculated by eqs 6–8 are summarized in Table 9. The dash-double-dot lines in Figures 2–4 denote the calculated isotherms from the n -layer BET equation.

The prediction of the n -layer BET equation was worse than those of the A–D equations except for the isotherm of Al₂O₃ at 293.2 K. Also, the deviations of the n -layer BET equation from the experimental isotherms on the Zeocarbon were larger than those of the A–D equation. Moreover, the n -layer BET equation was not appropriate for the prediction of the water vapor adsorption on zeolite 13X.

Conclusions

The adsorption equilibria of water vapor were measured at (293.2, 313.2, 333.1, and 353.1) K and pressures up to

2.1 kPa for Al₂O₃ and 2.3 kPa for zeolite 13X and Zeocarbon, respectively. The order of the adsorption capacity of water vapor was zeolite 13X, Zeocarbon, and Al₂O₃ except at 293.2 K and in the high-pressure region. And the isotherms of zeolite 13X and Zeocarbon were more favorable than those of Al₂O₃. The adsorption isotherms of water vapor on all the adsorbents used were type II isotherms at 293.2 K. The experimental equilibrium data of water vapor on Al₂O₃, zeolite 13X, and Zeocarbon were satisfactorily correlated with the A–D equation. Especially, the A–D equation with the Sips equation showed the smallest deviation of all the adsorbents in the experimental range.

However, the prediction of the adsorption equilibrium of water vapor by the *n*-layer BET equation was not satisfactory for the adsorbents used, especially for Zeocarbon and zeolite 13X.

Literature Cited

- (1) Huggahalli, M.; Fair, J. R. Prediction of Equilibrium Adsorption of Water onto Activated Carbon. *Ind. Eng. Chem. Res.* **1996**, *35*, 2071–2074.
- (2) Ryu, Y. K.; Lee, S. J.; Kim, J. H.; Lee, C.-H. Adsorption Equilibrium and Kinetics of H₂O on Zeolite 13X. *Korean J. Chem. Eng.* **2001**, *18*, 525–530.
- (3) Suzuki, M. *Adsorption Engineering*; Elsevier: Amsterdam, 1990.
- (4) Yang, R. T. *Gas Separation by Adsorption Process*; Butterworth: Boston, MA, 1987.
- (5) Lee, J. S.; Hong, J. S.; Suh, J. K.; Lee, C.-H.; Lee, M. S. Synthesis of zeolite X/activated carbon composite from rice hull. *Microporous Mesoporous Mater.*, accepted.
- (6) Lee, J. S.; Kim, J. H.; Kim, J. T.; Suh, J. K.; Lee, J. M.; Lee, C.-H. Adsorption Equilibria of CO₂ on Zeolite 13X and Zeolite X/Activated Carbon Composite. *J. Chem. Eng. Data*, accepted.
- (7) Aranovich, G. L.; Donohue, M. D. A New Approach to Analysis of Multilayer Adsorption. *J. Colloid Interface Sci.* **1995**, *173*, 515–520.
- (8) Do, D. D. *Adsorption Analysis*; Imperial College Press: London, 1998.

Received for review July 8, 2002. Accepted September 23, 2002.

JE0201267